JOURNAL OF MATERIALS SCIENCE 15 (1980) 2001–2009

The effect of nucleation density on the kinetics of crystallization and on the resulting structure and thermal properties of polymers crystallized during cooling

K. A. NARH, J. A. ODELL, A. KELLER, G. V. FRASER
H. H. Wills Physics Laboratory, University of Bristol, Royal Fort, Tyndall Avenue, Bristol UK

Following up the previous studies on this topic [1] it is verified that in the course of crystallization of polyethylene melts taking place during cooling, the number of predetermined nuclei initiating crystallization influences not only the scale of the spherulitic texture in the fully crystallized sample, but also the thickness of the lamellae and through it the melting behaviour of the final product and this in a predictable manner. Extending the scope of the previous study [1] these results were now obtained in samples in which the nucleation density was systematically altered, with all other relevant variables kept constant. The investigation thus demonstrates the previously unsuspected subtleties which can influence the structure and properties of samples which have been crystallized non-isothermally. It also provides an example for the complementary use of different techniques such as light scattering, optical microscopy, DSC calorimetry and Raman spectroscopy, for the purposes in question.

1. Introduction

This work is a follow-up of the study carried out in this laboratory between the period of 1977 to 1978 [1]. In this work Fraser *et al.* observed that different commercial samples of high-density polyethylene, with broadly similar molecular weight distributions and melt flow indices, after crystallizing under conditions of constant cooling rates, possessed widely varying melting points. Furthermore, these different melting points were found to be correlated with differences in spherulite size in the samples, which were in turn controlled by the density of nucleating heterogeneities. Below we briefly summarize the mechanism which was postulated to explain this effect.

During cooling from the melt the spherulites start to grow at a radial growth rate which increases with decreasing temperature. Clearly if the nucleation density is high the material will fully crystallize rapidly; conversely if the nucleation density is low completion of crystallization will take much longer. In terms of crystallization temperature (T_c), for a system crystallizing at a constant cooling rate, this means that samples with high nucleation density will crystallize, on average, at a higher temperature than those with a low nucleation density. This, in turn, affects the lamellar thickness of the polyethylene crystals, which itself governs the ultimate melting point.

The lamellar thickness L is related to the supercooling ΔT by [2, 3]

$$L = \frac{2\sigma_e T_m^0}{\Delta H_f \Delta T} + \delta L \qquad (1)$$

where σ_e is the fold surface free energy, ΔH_f is the heat of fusion, T_m^0 is the equilibrium melting temperature, and δL is a quantity arising from the kinetic theory which varies slowly with supercooling.

From Equation 1 we note that samples with lower supercooling are expected to have larger lamellar thickness. Expressing Equation 1 in terms of the melting temperature, T_m, we obtain

0022–2461/80/082001–09$02.90/0

$$T_m = T_m^0 \left(1 - \frac{2\sigma_e}{\Delta H_f L}\right) \quad (2)$$

neglecting the term δL.

It is clear from Equation 2 that samples with larger lamellar thickness should have higher melting points. Also, as the lamellar thickness is controlled by the spherulite size, and hence the nucleation density, it follows that the melting point will be controlled by the nucleation density. Thus the experimental observations in the preceding work could be explained by the simple theory of the kinetics of crystallization.

The correlation between the spherulite size and supercooling may also be expressed analytically. The radial growth rate of a spherulite G is related to the supercooling in the form [3]

$$G = G_0 \exp\left(-\frac{K}{T\Delta T}\right), \quad (3)$$

where G_0 and K are growth rate constants and T the growth temperature. When a material is crystallized at a set cooling rate ρ, the supercooling increases in proportion to an elapsed time, t. The growth rate as a function of time then becomes [1]

$$G = G_0 \exp - \left[\frac{K}{\rho t(T_m - \rho t)}\right]. \quad (4)$$

Substituting literature values of G_0 and K for polymers crystallizing within the narrow molecular weight fraction into Equation 4, a close fit was found between the theoretical and the experimental correlation relating the spherulite size and the temperature of maximum growth rate for identical cooling rates [1].

One of the obvious simplifications of the preceding work [1], is the assumption that all the samples have the same growth rate under identical conditions. Since the samples are of commercial type, one would expect some differences in the molecular weight distribution of each sample and this may affect the growth rate. Furthermore, the number of nucleating centres depended on the sources of the material in an arbitrary manner. Our main objective in the present work, therefore, is two-fold: (a) to measure the growth rate directly; (b) to vary the nucleation density in one and the same sample and test how far the conclusions of Fraser *et al.* [1] hold up under the more rigorously controlled and defined conditions. We found that the results from (a) show some variation in the growth rates of the samples [4]. Therefore, we selected only two samples for the experiments under (b) and the subsequent experiments parallel to those in the previous work [1] in order to test how far the effects observed there can be reproduced by controlled variation of the number of nucleating centres.

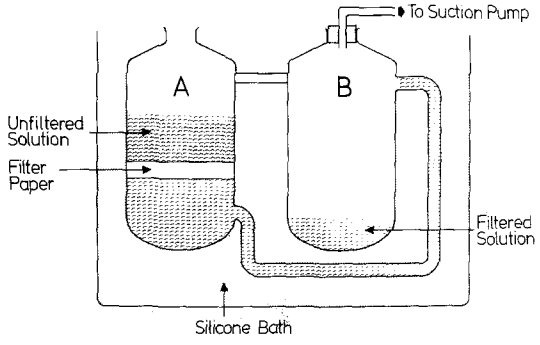

Figure 1 Schematic diagram of the filter system.

2. Experimental details

The two HDPE samples selected for this work have been previously labelled P and V [1] (see Table I). They have almost identical molecular weight distributions but differ significantly in their spherulitic textures. The nucleation densities of P and V spherulites were altered by (i) filtering out the heterogeneities which may have been introduced into the material deliberately or otherwise during manufacture from the sample of high

TABLE I

Sample	Molecular weight by GPC		Spherulite radius at room temp (μm) (by light scattering)	Nucleation density (cm^{-3}) for 8.1 mg
	$\bar{M}_w$	$\bar{M}_n$		
P(a-r)	61	10	9.0	2.76×10^6
P(f_{10})	46	10	12.4	1.06×10^6
P(f_2)	42	11	15.1	5.94×10^5
V(a-r)	65	11	47.0	1.94×10^4
V(+ 1% PS)	40	13	13.3	8.56×10^5

nucleus content (P) to reduce the number of nuclei, and by (ii) adding a nucleating agent to the sample of low nucleus content (V) in order to increase its nucleation density [4].

Having obtained samples with deliberately altered nucleation densities, we decided to repeat some of the experiments described in the earlier work [1]. These included the following techniques and measurements: small-angle light scattering for the measurement of the spherulite radii; optical microscopy for the assessment of the spherulitic textures; differential scanning calorimetry for the measurement of the crystallization rates, the extent of crystallization and the melting point; Raman spectroscopy for the measurement of the lamellar thickness.

2.1. Variation of nucleation density

2.1.1. Filtration of solution of sample P

A 0.5 wt% polyethylene solution was prepared by dissolving 2.5 g sample P in 500 ml boiling xylene heated by a magnetic stirrer hot plate. The solution was quickly transferred into a Corning filter bottle shown schematically in Fig. 1. A contains the filter paper and the freshly prepared hot polymer solution. B, which is connected to suction pump P, stores the filtered solution. Two grades of filters were used: grade 4 which has pore sizes ranging between 4 and 10 μm, and grade 5 with pore sizes of $< 4\,\mu$m.

Under the assumption that most nucleating agents are insoluble in the xylene [5] the solution was filtered hot in a thermostatically controlled silicon bath preset at 110° C. The filtrate was allowed to cool to room temperature before the solvent was drained off. The polymer was then washed in acetone and dried in a vacuum oven at 60° C. 24 h drying was sufficient to give solvent-free samples.

2.1.2. Addition of potassium stearate to sample V

In order to increase the nucleation density we added the nucleating agent [5] potassium stearate to sample V which had the coarsest spherulitic texture [1, 4]. The potassium stearate prepared from potassium hydroxide (KOH) and stearic acid ($CH_2(CH_2)_{16}COOH$) in a molar proportion of 1 : 1 and 1 wt% in water was incorporated into the polymer in the following manner. A quantity of the stearate was first powdered in a mortar until a microscopic examination showed average grain diameter of 3 μm. 1 wt% of it was then stirred into the polymer solution prepared from 0.5 wt% of the sample in xylene. The mixture was warmed on the magnetic stirrer hot plate at 40° C until the polymer began to crystallize. The solvent was then drained off and the polymer dried first in air for 12 h, and finally in the vacuum oven at 60° C for 24 h.

Before using the samples modified either by methods described in Section 2.1.1 or 2.1.2 for further experiments, checks for possible changes in molecular weight were made by gel permeation chromatography (GPC).

2.2. Measurement of spherulite size and growth rates

2.2.1. Small-angle light scattering (SALS)

Each sample weighing about 10 mg was melted between a microscope glass slide and a coverslip on a Kofler hot bench. The appropriate film thickness for light scattering was obtained by pressing the coverslip on to the sample until a film diameter of about 10 mm was obtained. At this diameter the film thickness was estimated to be about 80 μm. The sample was then held in a Mettler hot stage and its temperature raised to the melting point before being cooled at a chosen cooling rate down to room temperature.

The scattering apparatus was the same as that used previously [1]. It uses the highly collimated output of a helium–neon laser operating at 1 mW. The diameter of the beam was adjusted to about 4 mm, the size of the exit window of the hot stage. The specimen-to-film distance varied depending on the image size. The scattered light passed through an analyser and was recorded on photographic film with a 35 mm camera. As known, the method relies principally on the orientation anisotropy within the spherulites. In the case where the polarization direction of the analyser is perpendicular to that of the laser, the H_v configuration, a four-leaf clover pattern is formed. The scattering angle of maximum intensity (θ_m) within this pattern was obtained by scanning with a Joyce Loebl Microdensitometer, from which the spherulite radius (R) could be obtained through the relation

$$R = \frac{\lambda}{\pi \sin(\theta_m/2)}, \qquad (5)$$

where λ is the wavelength of the incident light. The value of λ used was 632.8 nm [6].

2.2.2. Optical microscopy (OM)

The spherulitic textures of the samples were also assessed by optical microscopy under crossed polars. Photomicrographs were taken of the samples crystallized at a cooling rate of 10° C min^{-1}. Each sample was held between a microscope slide and a coverslip and initially melted on the Kofler hot bench. The sample was then introduced into the Mettler hot stage and its temperature raised at 10° C min^{-1} to about 5° C above its melting point. After complete melting the temperature was lowered at the same rate to room temperature.

2.2.3. Differential scanning calorimetry (DSC)

In addition to the SALS and OM measurements of the spherulite sizes, the nucleation densities as well as the radial growth rates of the five samples were also determined indirectly from the crystallization rate measurements.

The crystallization rates of the samples were determined with a Perkin–Elmer Differential Scanning Calorimeter (DSC 2). Each specimen was heated to 143° C at a rate of 20° C min^{-1} and allowed to remain there for 3 min to ensure that melting was complete. The DSC was then set at the required crystallization temperature (T_c) and the sample cooled as fast as possible to this temperature. The thermogram was recorded when both the sample and DSC chambers have attained thermal equilibrium. The radial growth rate of the spherulites, G, was calculated from the DSC thermograms as follows. Let the volume of each spherulite be

$$V = \tfrac{4}{3}\pi r^3 \tag{6}$$

where r is the spherulite radius at any instant. The mass of material which has crystallized at any instant per unit volume, assuming instantaneous nucleation, is given by

$$m = \tfrac{4}{3}\pi r^3 \rho_c N \tag{7}$$

where N is the number of nucleating centres in a unit volume of material and ρ_c is the crystalline density. But $r = Gt$, where G is the radial growth rate and t is time, therefore

$$m = \tfrac{4}{3}\pi G^3 t^3 \rho_c N \tag{8}$$

so that the amount of material that has crystallized per unit time

$$\frac{dm}{dt} = 4\pi G^3 t^2 \rho_c N \frac{M}{\rho_s}, \tag{9}$$

where M and ρ_s are the mass and density, respectively. Hence a plot of dm/dt against t^2 gives a slope $\bar{g}$ given by

$$\bar{g} = 4\pi G^3 N M \rho_c / \rho_s$$

or

$$N = \frac{\bar{g}\rho_s}{4\pi G^3 M \rho_c}. \tag{10}$$

Also if the final spherulite radius is R, the final spherulite volume $V_f = \frac{4}{3}\pi R^3$ and N is given by

$$N = \frac{1}{V_f} = \frac{3}{4\pi R^3}. \tag{11}$$

Combining Equations 10 and 11 we get

$$G = R\left(\frac{\bar{g}\rho_s}{3M\rho_c}\right)^{\frac{1}{3}}, \tag{12}$$

from which G may be obtained.

We must point out that only the first part of the DSC curve can be used before the impingement of the spherulites restricts the growth rates.

2.3. Measurement of crystallization temperature (T_c) (supercooling ΔT)

On crystallization during cooling there is a particular temperature where the rate of crystallization has a maximum value, which will be referred to as the crystallization temperature T_c, with $T_m - T_c$ (ΔT) as the corresponding supercooling. T_c (or ΔT) thus defined can be identified with that of the exotherm peak in the corresponding DSC thermogram recorded during cooling.

According to our earlier work [1] this T_c decreases with increasing rate of cooling but at a fixed cooling rate T_c is higher (ΔT lower) for samples with higher nucleation density. We repeated this experiment with our five samples.

About 8 mg of each specimen was prepared in the usual manner for use in the DSC. The sample was heated at the rate of 5° C min^{-1} from room temperature to 143° C and kept at this temperature for 3 to 4 min. The temperature was then lowered at the required cooling rate and the DSC peak recorded as the temperature at which the crystallization rate reaches its maximum.

2.4. Measurement of the lamellar thickness (L)

Each sample was crystallized in the DSC (at a fixed heating and cooling rate) as described in Section 2.3. The sample was then removed from the DSC pan for the Raman spectroscopy. We used

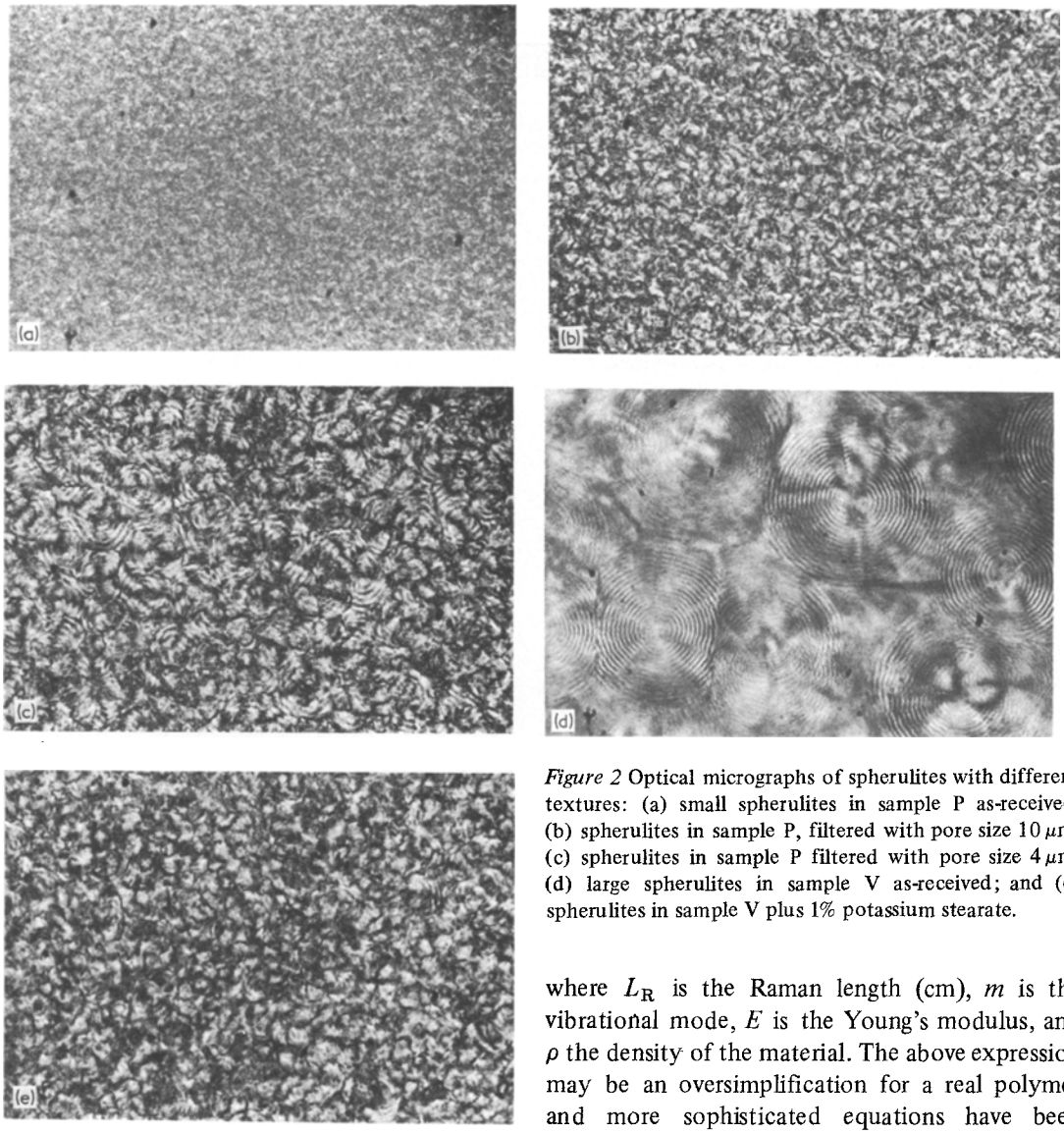

Figure 2 Optical micrographs of spherulites with different textures: (a) small spherulites in sample P as-received; (b) spherulites in sample P, filtered with pore size 10 μm; (c) spherulites in sample P filtered with pore size 4 μm; (d) large spherulites in sample V as-received; and (e) spherulites in sample V plus 1% potassium stearate.

a Coderg T800 Raman spectrometer and a krypton ion laser operated at 530.9 nm to excite the spectra.

To recapitulate, the Raman spectroscopy utilizes the phenomenon of inelastic scattering of light by the molecules which gives rise to a peak corresponding to the longitudinal acoustic model (LAM) at a frequency slightly shifted from that of the exciting radiation. The frequency shift $\Delta\tilde{\nu}$ in wave numbers (cm^{-1}) of the LAM peak is given by [7]

$$\Delta\tilde{\nu} = \frac{m}{2L_R}\sqrt{\left(\frac{E}{\rho}\right)} \qquad (13)$$

where L_R is the Raman length (cm), m is the vibrational mode, E is the Young's modulus, and ρ the density of the material. The above expression may be an oversimplification for a real polymer and more sophisticated equations have been proposed [8]. In this paper we have used Raman chain lengths calculated from Equation 13 for comparative purposes rather than for making structural conclusions from absolute values.

3. Results and discussion

Table I gives the summary of the average spherulite radii together with the weight average and number average molecular weights. The following symbols have been employed to identify each of the samples: P(a-r) = P as-received; $P(f_2)$ = P filtered, approximate pore size 2 μm; $P(f_{10})$ = P filtered, approximate pore size 10 μm; V(a-r) = V as-received; V(+ 1% PS) = V + 1% potassium stearate.

The effect of filtration and the addition of potassium stearate to the sample is pronounced.

Column 3 of the table shows that significant changes occurred in the spherulite sizes from P(a-r) through P(f_2), in the expected direction. That is, the smaller the pore size of the filter the fewer the heterogeneities that remained in the material after filtration and hence the lower the nucleation density. The changes in V also fall in line, the effect being a decrease in the spherulite size and hence an increase in the nucleation density with the addition of nuclei.

On the whole, the results in Table I do not indicate any significant changes in the molecular weight distribution resulting from the preparation techniques. We ascribe any apparent differences in the table to the uncertainty in the GPC measurements which is sometimes as high as $\pm 10^4$ in 10^5 $\bar{M}_w$ for the same material. This is probably due to the fact that the GPC is not very sensitive in the high molecular weight tail.

The variation of the spherulite size is directly apparent from the optical microscope image. Fig. 2a to e show the changes which occurred in the virgin material as its nucleation density has been altered.

The optical microscopy yields spherulite sizes which appear smaller than obtained by SALS in Table I. This is the general impression one gets from optical microscopy of spherulites and we attribute this effect to the sample thickness. For a thicker sample there is the possibility of one viewing the spherulites which overlay those inside the material and thus getting the impression of a finer texture than is actually the case. The SALS technique, on the other hand, gives a more representative result and is therefore more reliable.

Fig. 3a shows a typical DSC thermogram for isothermal crystallization at $T_c = 118^\circ$ C for sample P(a-r). The sigmoidal curve in Fig. 3b represents the percentage of the material crystallized as a function of time. This curve was obtained by taking the ratio of the area under the curve in Fig. 3a at any instant, to the total area at the end of crystallization and plotting this as a function of time. It is the inflexion point of the curve in Fig. 3b which corresponds to the exotherm peak of the DSC curve and it is this which gives the maximum rate of crystallization which also corresponds to the point where the spherulites begin to impinge.

Fig. 4 shows plots of dm/dt against t^2 for the five samples at $T_c = 118^\circ$ C. From these plots, the SALS measurement of the spherulite radii and the masses of the samples, the radial growth rates G were obtained by Equation 12 for $T_c = 118, 120,$ 122 and 124° C. Table II is a summary of the measurements described in Section 2.2.3.

From Equation 12, for a constant growth rate G at a particular crystallization temperature one would expect the ratios $(R_1/R_2)^3$ and $(\bar{g}_2 M_1/\bar{g}_1 M_2)$ to be equal, the subscripts 1 and 2 representing the virgin sample and the sample whose nucleation density has been varied, respectively. Two columns in Table II, under appropriate headings, show the correlation between these two ratios. It is clear from the table that the two ratios at the same T_c, for all practical purposes, are

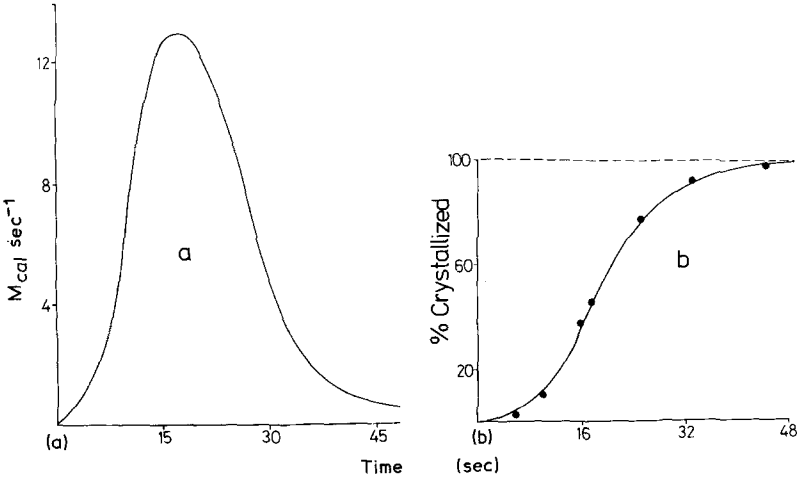

Figure 3 (a) A typical DSC thermogram of sample P as-received, $T_c = 118^\circ$ C. (b) A sigmoidal crystallization curve obtained from (a). Consult text for details of derivation.

TABLE II

Sample	Mass (mg)	Isothermal crystallization temperature (° C)	Final spherulite radius (μm)	Slope $\bar{g}$ (g sec^{-3})	$\left(\frac{R_1}{R_2}\right)^3$	$\frac{\bar{g}_2 M_1}{g_1 M_2}$	Radial growth rate (μ m sec^{-1})
P(a-r)	8.1	118	9	1.34×10^{-6}	1	1	0.340
	8.1	120	9	2.68×10^{-7}	1	1	0.200
	8.1	122	9	6.00×10^{-9}	1	1	0.057
	8.1	124	9	4.70×10^{-11}	1	1	0.011
P(f_{10})	7.1	118	12.4	4.18×10^{-7}	2.62	2.81	0.334
	7.1	120	12.4	8.72×10^{-8}	2.62	2.69	0.199
	7.1	122	12.4	2.84×10^{-9}	2.62	2.43	0.063
	7.1	124	12.4	1.55×10^{-11}	2.62	2.71	0.011
P(f_2)	7.8	118	15.1	2.54×10^{-7}	4.72	4.93	0.334
	7.8	120	15.1	3.49×10^{-8}	4.72	7.40	0.171
	7.8	122	15.1	1.66×10^{-9}	4.72	5.10	0.062
	7.8	124	15.1	9.03×10^{-12}	4.72	5.11	0.011
V(a-r)	6.7	118	47	4.62×10^{-8}	1	1	0.620
	6.7	120	47	2.70×10^{-9}	1	1	0.241
	6.7	122	47	5.77×10^{-11}	1	1	0.071
V(+ 1% PS)	5.6	118	13.3	1.33×10^{-6}	47.3	34.0	0.570
	5.6	120	13.3	7.69×10^{-8}	47.3	34.1	0.221
	5.6	122	13.3	2.17×10^{-9}	47.3	38.3	0.067

constant for samples of the same material but differ significantly for samples of different materials. The growth rates also follow similar trends. Thus the structural and physical properties of samples from the same material appear to depend only on the nucleation density, which is the only variable parameter in this experiment.

The slight difference in the growth rates in column 8 of Table II can be ascribed to certain inherent errors, such as (1) the slight variation in the molecular weight distribution among the various samples, and (2) the uncertainty in the "zero time" (i.e. the time at which crystallization begins) and the uncertainty in the baseline determination of the DSC curves. The uncertainty in the zero time is very much dependent on the temperature of crystallization; the lower the T_c the faster the rate of crystallization and hence the more difficult it becomes to determine the zero time. In spite of these experimental uncertainties, however, the results point to one main fact: the nucleation density is the only factor which is responsible for the differences between polymers of identical molecular weights and growth rates arising under otherwise identical cooling conditions.

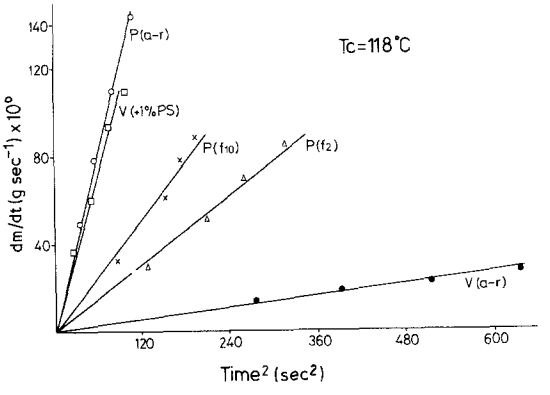

Figure 4 Experimental correlation between crystallization rates and nucleation densities. Consult text for details.

Fig. 5 shows the variation of the crystallization temperatures with cooling rates. This result confirms that of Fraser *et al.* [1] and shows a clear correlation between the nucleation density, in this instance varied within the same material, and the crystallization temperature. Fig. 5 reveals that samples with higher nucleation densities also have higher crystallization temperatures over a range of cooling rates. Using a fixed cooling rate, Table III shows the dependence of melting and crystallization temperatures on the nucleation density. It is seen that for samples of the same

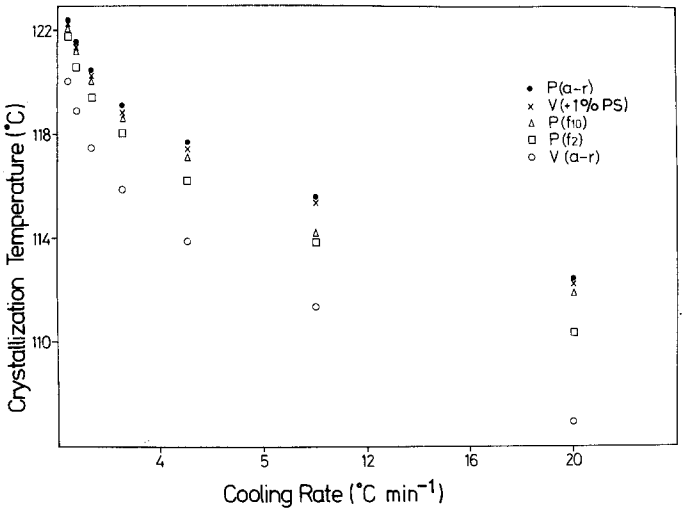

Figure 5 Experimental correlation between cooling rate and crystallization temperature T_c (temperature at which the crystallization rate is fastest).

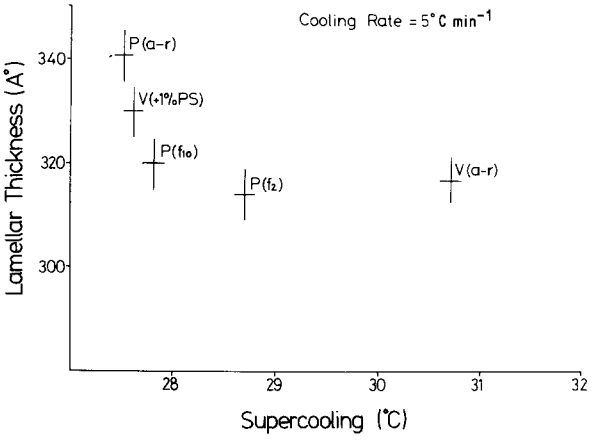

Figure 6 Experimental correlation between Raman lamellar thickness L_R and supercooling (ΔT).

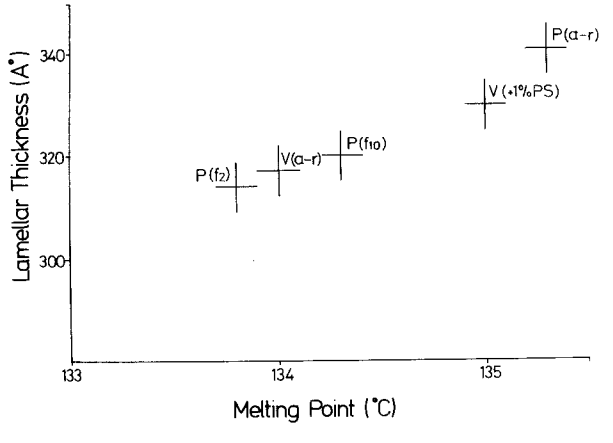

Figure 7 Experimental correlation between Raman lamellar thickness and melting point (T_m).

TABLE III

Sample	Nucleation density (cm^{-3}) for 8.1 mg	Crystallization temperature (° C) (cooling rate 5° C min^{-1}) (DSC exotherm peak)	Melting temp. (° C) (heating rate 5° C min^{-1}) (DSC endotherm peak)
P(a-r)	2.76×10^6	117.5	135.3
P(f_{10})	1.06×10^6	117.2	134.3
P(f_2)	5.94×10^5	116.2	133.8
V(a-r)	1.94×10^4	113.9	134.3
V(+ 1% PS)	8.56×10^5	116.9	135.1

material both the crystallization temperatures and melting points are higher for higher nucleation densities.

Fig. 6 shows the experimental correlation between the lamellar thickness and supercooling and Fig. 7 that between the lamellar thickness and the melting point. The general trend of these figures is in accord with the theoretical expectation (Equation 12) and confirm the previous results [1], but now obtained under conditions of controlled nucleation density within the same samples where the isothermal spherulite growth rates were separately ascertained and verified to be constant.

4. Conclusions

We have demonstrated how the nucleation density influences the texture and thermal properties of polyethylene crystallized during cooling. By deliberately altering the nucleation density, while keeping the growth rate and molecular weights constant, we were able to study the conditions under which these differences in texture and properties occur. It is now clear that at a constant spherulite growth rate the resulting effective crystallization temperature, lamellar thickness and subsequent melting behaviour will depend only on the nucleation density, a fact already acknowledged by Fraser *et al.* [1]; however, without independent control of the parameters involved, a control the present study has introduced.

We believe the results of this work are relevant to the solidification and to the control of the resulting texture and properties of technological material obtained by melt processing wherever the material solidifies during cooling.

Acknowledgements

We would like to thank Mrs A. Halter for carrying out the GPC analyses. K.A.N. would also like to thank the Ghana Government for financial support.

References

1. G. V. FRASER, A. KELLER and J. A. ODELL, *J. Appl. Polymer Sci.* **22** (1978) 2979.
2. J. D. HOFFMAN and J. I. LAURITZEN, Jr. *Appl. Phys.* **44** (1973) 4340.
3. F. C. FRANK and N. TOSI, *Proc. Roy. Soc.* **A263** (1961) 323.
4. K. A. NARH, M.Sc. Thesis, University of Bristol (1978).
5. F. L. BINSBERGEN, *Polymer* **11** (1970) 253.
6. R. S. STEIN and M. B. RHODES, *J. Appl. Phys.* **31** (1960) 1873.
7. S. L. MIZUSHIMA and T. SHIMANOUCHI, *J. Amer. Chem. Soc.* **71** (1949) 1320.
8. S. L. HSU and S. KRIMM, *J. Appl. Phys.* **48** (1977) 4013, and other references therein.

Received 14 November and accepted 8 January 1980.